

# Amorphous Silicon Carbide Rear-Side Passivation and Reflector Layer Stacks for Multi-Junction Space Solar Cells based on Germanium Substrates

<sup>1</sup>Stefan Janz, <sup>1</sup>Charlotte Weiss, <sup>1</sup>Christian Mohr, <sup>2</sup>Rufi Kurstjens, <sup>3</sup>Bruno Boizot, <sup>4</sup>Bianca Fuhrmann and <sup>4</sup>Victor Khorenko

<sup>1</sup>Fraunhofer Institute for Solar Energy Systems, Freiburg, 79110, Germany; <sup>2</sup>Umicore Electro-optic Materials, Watertorenstraat 33, 2250 Olen, Belgium; <sup>3</sup>Laboratoire des Solides Irradiés, CNRS-UMR 7642, CEA- DRF-IRAMIS, Ecole Polytechnique, Université Paris-Saclay, Palaiseau Cedex, 91120, France; <sup>4</sup>AZUR SPACE Solar Power GmbH, Theresienstr. 2, 74072 Heilbronn, Germany

**Abstract** — New developments for space solar cells mainly address efficiency improvements and weight reduction. In this paper we developed amorphous SiC based layer stacks for passivation and enhanced reflection on thin and lowly doped ( $2 \times 10^{16}$  -  $1 \times 10^{17}$  at/cm<sup>3</sup>) Ge wafers. Passivated Ge samples with minority carrier lifetimes of more than 300  $\mu$ s and surface recombination velocities of just 17 cm/s are presented. Thermal annealing at 400 °C and additional “mirror” layer deposition do not harm the minority carrier lifetimes or lead to an even slight increase. Electron irradiation with fluences of  $1 \times 10^{15}$  e/cm<sup>2</sup> and more lead to strong material degradation and lifetimes of just 5  $\mu$ s.

## I. INTRODUCTION

Recent developments in space solar cell research are focusing on higher efficiencies and thinner cells to increase the power-to-weight (W/g) ratio [1]. In addition, the End-Of-Life performance is important especially for satellites using electric orbit raising technology. The latter technology results in a higher radiation load during the transfer time of the satellite [2]. Today’s state-of-the-art technology for space is a triple-junction GaInP/GaInAs/Ge cell in which the Ge bottom cell generates a significant excess current. A promising candidate for the next generation space solar cells is a four-junction metamorphic device with a Ge bottom sub-cell [3] in which all junctions are current matched. It is therefore important to understand how the photocurrent in the Ge bottom cell can be increased and how it reacts to the radiation environment in space. In order to increase the current generated by the longer wavelength photons, the bulk minority carrier lifetime needs to be increased. Furthermore applying a mirror layer to the back surface of the Germanium is needed in order to significantly enhance the light path and absorption in this wavelength range. This is especially important as Germanium is an indirect semiconductor with low absorption between 1600-1850 nm. Besides that such a mirror reflects photons with energy below the bandgap back into space which allows reaching lower cell operating temperatures and therefore higher efficiency.

In this paper we are investigating layer stacks of amorphous silicon carbide (a-Si<sub>x</sub>C<sub>1-x</sub>:H / a-SiC:H) which should provide

both, excellent surface passivation and enhanced reflection beyond 1800 nm (see Fig. 1). In order to investigate the right combination of diffusion length of carriers, passivation performance and current generation in the Ge we fabricate wafers in a wide doping range from  $2 \times 10^{16}$  at/cm<sup>3</sup> to  $1 \times 10^{17}$  at/cm<sup>3</sup>. The investigations of plasma cleaning and passivation are discussed and compared to literature values [2, 3]. Furthermore post processing like thermal annealing and accelerated aging with electrons is investigated.

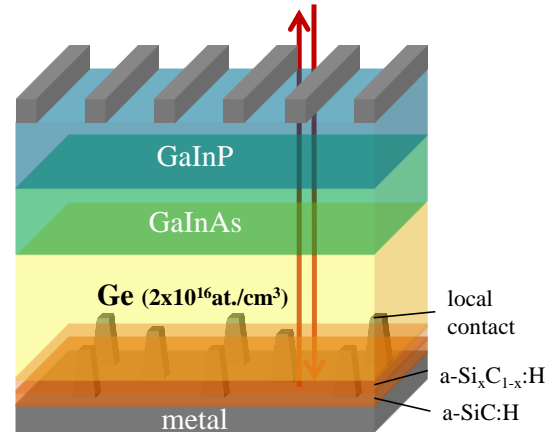


Fig. 1. Lattice-matched triple-junction solar cell with a-Si<sub>x</sub>C<sub>1-x</sub>:H / a-SiC:H back side structure for excellent surface passivation and enhanced reflection including local contact points.

## II. EXPERIMENTAL

Dislocation free Czochralski pulling of Ge substrates for solar cells is a well-established technology. However, most activities have been focusing on the doping range of interest for lattice matched triple-junction cells ( $1 \times 10^{17}$  –  $1 \times 10^{18}$  at/cm<sup>3</sup>) with a process optimization towards stable and uniform doping throughout the crystal. In order to investigate which doping range is optimal, a crystal with a doping gradient was pulled in the frame of this work. Taking wafers from such an ingot allows an investigation of different doping concentrations where all wafers have otherwise similar crystal quality. Ge ingots were pulled with a target gradient in doping

from  $1 \times 10^{16} - 1 \times 10^{17}$  at/cm<sup>3</sup> enabling good material quality over a wide doping range. Out of these ingots 4” wafers with thicknesses from 150 to 650  $\mu\text{m}$  were produced.

After the pre-conditioning and shipping of the wafers they were unpacked and stored for one day under clean-room conditions to allow a reproducible oxidation of the surface. This step is necessary to avoid undefined surface conditions of the samples depending on the interval between unpacking and subsequent processing. In this way, a reasonable comparison and analysis of the passivation quality of different Ge samples should be assured. Depending on further processing some 4” wafers were broken or cut into smaller pieces simply to allow for efficient use of the precious material.

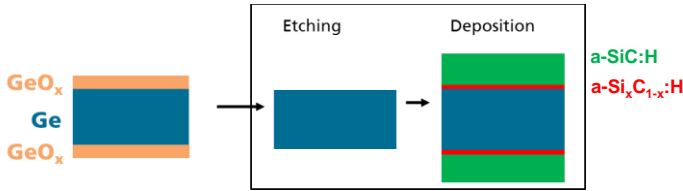


Fig. 2. Process flow for the symmetrically processed “lifetime” samples starting with the oxidized Ge wafer, the plasma etching, the passivation ( $\text{a-Si}_x\text{C}_{1-x}\text{:H}$ ) and mirror layer ( $\text{a-SiC:H}$ ) deposition.

The removal of the oxide formed on the Ge surface was done by a dry etching step under vacuum conditions inside a plasma enhanced chemical vapor deposition (PECVD) reactor using a  $\text{H}_2/\text{Ar}$  gas mixture. The exposure time of this etching process has to be carefully optimized to achieve (i) a complete removal of the native oxide on the Ge surface without (ii) damaging the Ge surface. The plasma cleaning process duration for oxygen removal was varied between 0 and 50 s. In an in-situ process an amorphous silicon carbide  $\text{a-Si}_x\text{C}_{1-x}\text{:H}$  layer (passivation layer) with ( $x \approx 0.95$ ) was deposited using methane ( $\text{CH}_4$ ), silane ( $\text{SiH}_4$ ) and hydrogen ( $\text{H}_2$ ) as precursor gases at a temperature of 270  $^\circ\text{C}$ . For some samples the second stoichiometric  $\text{a-SiC:H}$  layer (“mirror” layer) was deposited in-situ using the same precursors. As for further solar cell processing p-doping of the film is essential,  $\text{H}_2$  is substituted by diborane ( $\text{B}_2\text{H}_6$ ) in order to dope the layers (see Fig. 2). Associated to plasma related processes we focused on the investigation of the plasma pre-conditioning of the Ge surface. In addition to that the temperature stability of the passivation layers was tested by exposing it to an annealing step on a hotplate at air ambient between 400  $^\circ\text{C}$  and 500  $^\circ\text{C}$  for 5 to 30 min. These thermal budgets are representative for further processes like e.g. metal/Ge contact annealing (400  $^\circ\text{C}$ ). The prepared Ge samples for lifetime evaluation were processed exactly the same way on both sides (see Fig. 2).

The electrical quality of the surface passivation layer was characterized using microwave-detected photoconductance decay ( $\mu\text{PCD}$ ) [4] technique which is a purely transient method measuring the exponential decay of excess carriers immediately after a short laser illumination. In this system, a

short laser pulse (904 nm) on top of a steady state bias light generates excess carriers within the investigated wafer. This leads to an increase of the wafer conductance. After termination of each pulse, the excess carriers diffuse and recombine within the bulk and at both surfaces of the wafer and the photo-conductance decreases exponentially to its initial value. For the detection of the conductance, microwaves generated in a phase-locked microwave oscillator are directed through a waveguide and the reflected microwaves are redirected towards the detector. Depending on the sample conductance, the signal is reflected with varying intensity. The time dependence of this quantity is recorded by a digital storage oscilloscope and then analyzed.

The measured minority carrier lifetime  $\tau_{\text{eff}}$  is an effective differential lifetime combining the carrier lifetime within the bulk  $\tau_{\text{bulk}}$  and a surface carrier lifetime, characterized by the parameter surface combination velocity ( $S_{\text{eff}}$ ):

$$\frac{1}{\tau_{\text{eff}}} = \frac{1}{\tau_{\text{bulk}}} + \frac{1}{\tau_{\text{surface}}} = \frac{1}{\tau_{\text{bulk}}} + \frac{2}{W} \times S_{\text{eff}}. \quad (1)$$

For this experiment we varied the Ge wafer thickness (150  $\mu\text{m}$ , 300  $\mu\text{m}$  and 500  $\mu\text{m}$ ) and plotted the inverse effective differential lifetime versus two divided by the thickness  $W$  of the wafer to easily determine the carrier bulk lifetime as y-axis intersection and the surface recombination velocity  $S_{\text{eff}}$  as slope of the applied fit.

Finally, electron accelerated ageing at different fluences was done. For these experiments the “lifetime” samples were coated with three different mirror layers in order to investigate if the radiation damage can be influenced by them. Two batches with intrinsic mirror layers 100 nm or 200 nm thick and a third batch with a doped mirror layer (200 nm) were prepared. After annealing all wafers (4”) were cut to pieces of 20x20 mm<sup>2</sup>. For this irradiation campaign, the electron 1 MeV beam surface on the sample was a 26 mm diameter disk measured on a microscope glass lamella using a circular 23 mm diaphragm before the window of the irradiation chamber. During the irradiation, the sample and diaphragm currents were recorded and the electron charge at the back of the sample using an ORTEC integrator was integrated. The sample temperature was around 17  $^\circ\text{C}$ . In total more than 100 samples were irradiated between  $3 \times 10^{13}$  and  $10^{16}$  e/cm<sup>2</sup>. All irradiated samples were measured before and after irradiation in order to analyze the changes in the effective minority carrier lifetimes ( $\tau_{\text{eff}}$ ) as a function of the total electron fluence.

### III. RESULTS AND DISCUSSION

The current crystal pulling hardware and process is optimized towards reducing the doping gradient within one crystallization run. Some of the process steps could be modified to increase the gradient but still a second crystal had

to be pulled to be able to provide enough material. The first crystal that was pulled (cz102/803) had a steep gradient but a doping range that was above target (see Fig. 3). Some parts of this crystal (from head to middle) were used to supply wafers with doping concentration in the range of  $1 \times 10^{17}$  at/cm<sup>3</sup>. The second crystal that was pulled (cz102/804) had the same steep gradient and followed the target more closely. Material from this ingot was used to supply wafers of  $2 \times 10^{16}$  at/cm<sup>3</sup> and  $5 \times 10^{16}$  at/cm<sup>3</sup>. For further experiments we merged wafers into three doping categories (“high”  $9.7 \times 10^{16}$ - $1.1 \times 10^{17}$ , “middle”  $5.2$ - $6.2 \times 10^{16}$ , “low”  $\approx 2.3 \times 10^{16}$  at/cm<sup>3</sup>).

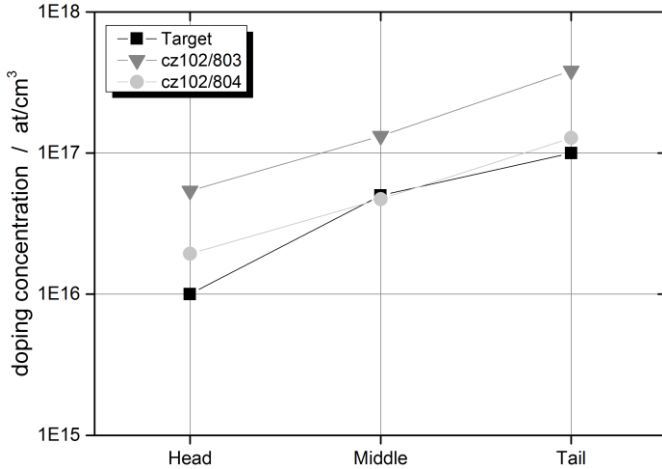


Fig. 3. Overview of the doping target and results for the two Ge crystals pulled (grey) including the target values (black).

The normalized minority carrier lifetime values for Ge samples of all three doping categories cleaned with the Ar/H<sub>2</sub> plasma are presented in Fig. 4.  $\tau_{\text{eff}}$  improves with reduced bulk doping concentration which is not surprising considering stronger Auger recombination contribution with increasing dopant concentration. Furthermore the values clearly improve with longer plasma exposure. This parallel behavior for all doping levels can be explained with an advancing removal of the oxide layer up to process durations of 30 s. The saturation or even a slight decrease in lifetimes can be due to starting bulk damage for even longer exposure times. However, this damage behavior can be concluded from the data for the lowly doped samples only. In contrast to this results Fernandez *et al.* [5] presented a much stronger degradation of passivation performance with longer plasma exposure. So far it is not clear why, with comparable plasma parameters and using the same reactor the samples presented here seem to show almost no plasma related bulk damage effects. Either a plasma generator adaptation in between the experiments leads to “softer” plasma with lower energy densities in the current setup or the oxidized Ge surfaces differ significantly in composition and/or thickness.

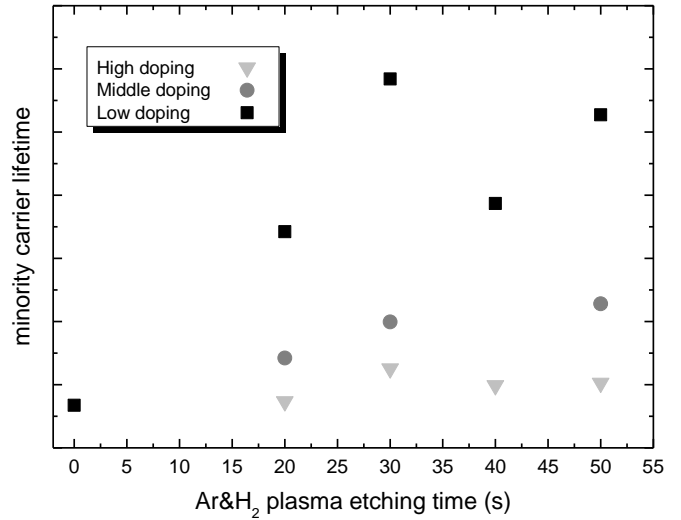


Fig. 4. Relative changes in minority carrier lifetimes of Ge samples with different doping concentrations after plasma cleaning and passivation with 30 nm of a-Si<sub>x</sub>C<sub>1-x</sub>:H on both sides of the wafer.

Based on the cleaning experiments a plasma exposure of >30 s was set for all following deposition experiments. The effective lifetime values for all three doping levels of Ge can be found in Fig. 5. From [5] we know that maximum effective lifetimes of 200  $\mu$ s for highly and 400  $\mu$ s for lowly doped Ge wafers can be expected. Measured lifetimes of  $\tau_{\text{eff}} > 300 \mu$ s for the lowly doped samples are the best lifetime values reported so far on such Ge wafers and proof that cleaning and passivation procedure are performing very well.

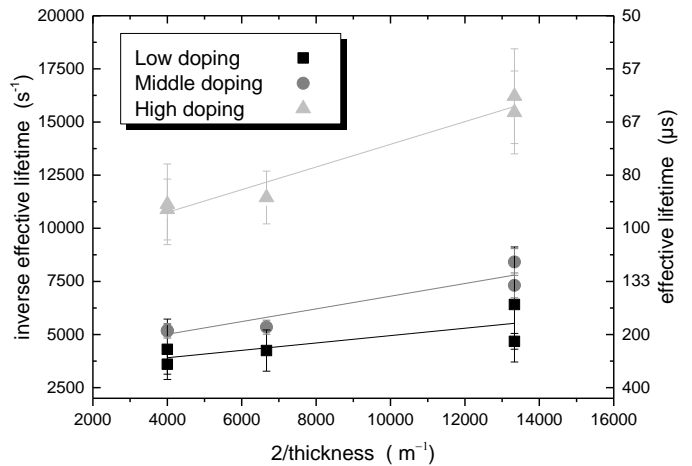


Fig. 5. Inverse effective lifetime versus 2/thickness for three different Ge doping levels and three wafer thicknesses of 150  $\mu$ m – 500  $\mu$ m (right to left).

Plotting the inverse effective differential lifetime versus two divided by the thickness  $W$  of the wafer (see Fig. 5) leads to carrier bulk lifetimes of 116  $\mu$ s, 261  $\mu$ s and 311  $\mu$ s, respectively. Surface recombination velocities  $S_{\text{eff}}$  of 17 to

53 cm/s (see Table 1) confirm the excellent passivation performance of the a-Si<sub>x</sub>C<sub>1-x</sub>:H layer. So far it is not clear why the  $S_{eff}$  values are increasing with doping level, but higher defect concentrations and/or other band structures at the interface are possible explanations.

Table 1 Bulk lifetime and surface recombination velocity for the three doping levels.

Doping level (at/cm <sup>3</sup> )	$\tau_{bulk}$	$S_{eff}$ (cm/s)
$2 \times 10^{16}$	311	17
$5 \times 10^{16}$	261	30
$1 \times 10^{17}$	116	53

After an annealing of samples at the maximum temperature of 500 °C for more than 5 min the minority carrier lifetimes are reduced by around 100  $\mu$ s. As blistering is observed, which is typical for hydrogen effusion from amorphous hydrogenated layers, we suppose that this out-diffusion of hydrogen is the reason for the degradation. We can therefore conclude that using already passivated Ge substrates for the epitaxial growth of the III-V top absorber layers seems to be impossible due to the degradation of the passivation performance with temperatures of  $\geq 500$  °C. However, in the further solar cell process the maximum temperature applied will be much below 500 °C. Therefore we annealed parallel samples at just 400 °C, which is e.g. a standard temperature for contact annealing. The minority carrier lifetimes for all three doping levels are (after 15 min), within the accuracy of the measurement, unchanged compared to not annealed samples.

In Fig. 6 a  $\mu$ PCD mapping of two lowly doped 4" wafers with passivation and additional stoichiometric a-SiC:H layers (mirror layers) are shown. The mirror layers are 200 nm thick and during deposition diborane was added for the sample on the right. After annealing at 400 °C some inhomogeneities of  $\tau_{eff}$  values over the wafers can be found. As plasma process inhomogeneity below 10 %, at least for the deposition, could be proven by ellipsometry measurements of the layers' thicknesses we think that the surrounding ring can be explained by edge effects (measurement artefacts). Other regions with lower lifetime values show tweezer prints and other handling traces. Further features like the ring-shaped structures on the wafer could have their origin in deviations of the bulk quality or dopant inhomogeneities in the bulk. For solar cell integration it is important to note that the additional mirror layer deposition leads to no degradation of the lifetime values ( $\tau_{eff} > 300$   $\mu$ s). In addition to that we find even increased lifetime values for the sample with the boron doped

mirror layers (see Fig. 6, right). One possible explanation could be the higher amount of charges in the doped layers leading to field effect passivation. However, so far it is not clear if saturation of dangling bonds or any charge related effect are leading to the excellent passivation performance of the a-Si<sub>x</sub>C<sub>1-x</sub>:H layers on Ge. Charging experiments and the measurement of surface voltage are needed to further investigate this point.

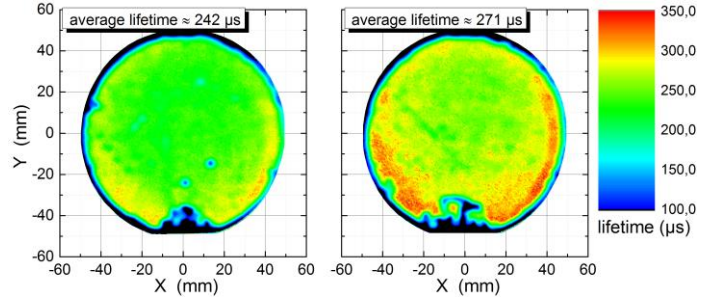


Fig. 6.  $\mu$ PCD mappings of two different 4" Ge wafers (doping concentration  $\approx 2 \times 10^{16}$  cm<sup>-3</sup>) after plasma cleaning, passivation with a-Si<sub>x</sub>C<sub>1-x</sub>:H, coating with stoichiometric intrinsic SiC:H (left) and p-doped SiC:H (right) and annealing.

As expected the electron irradiations show an increasingly detrimental effect on the samples' lifetimes with increasing fluences for all three doping levels of Ge (Fig. 7). The lowest total fluence of  $3 \times 10^{13}$  e/cm<sup>2</sup> reduces the lifetime from 206  $\mu$ s, 118  $\mu$ s and 54  $\mu$ s to 181  $\mu$ s, 100  $\mu$ s and 41  $\mu$ s for the three doping levels. Until a total fluence of  $3 \times 10^{14}$  e/cm<sup>2</sup> the three doping levels can still be distinguished from each other (34  $\mu$ s, 19  $\mu$ s and 12  $\mu$ s) but for  $1 \times 10^{15}$  e/cm<sup>2</sup> and  $1 \times 10^{16}$  e/cm<sup>2</sup> all three doping levels show the same lifetime values of 5  $\mu$ s and 2  $\mu$ s, respectively. We could find no influence of passivation layer thickness or doping level on the lifetime values after irradiation which leads to the conclusion that doping levels in Ge alone determine the radiation hardness of the structure. So far it is not clear which fluences have to be considered in order to represent the launching conditions through Van-Allen's belt and if the Ge bulk can regenerate under irradiation (photon annealing). However, as mobilities in Ge are very high even lifetimes of just 5  $\mu$ s in lowly doped material correspond to diffusion lengths for minority carriers of around 200  $\mu$ m. With a final Ge wafer thickness in the range of 70  $\mu$ m this can still lead to a significant efficiency improvement in the final solar cell.

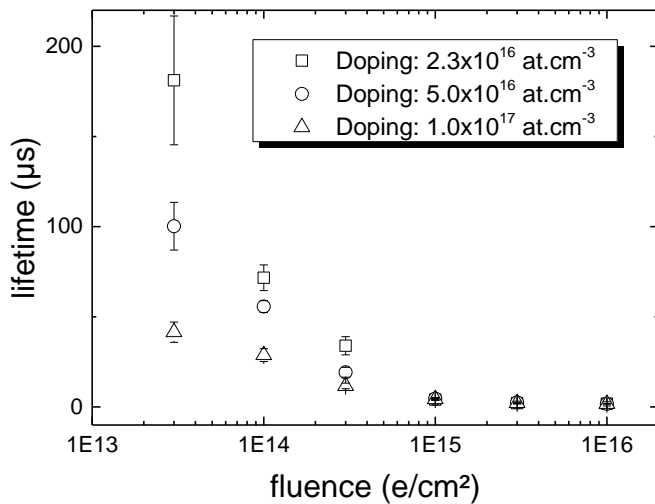


Fig. 7. Influence of electron irradiation on the lifetime degradation for the three different Ge doping levels.

#### IV. CONCLUSIONS

We investigated bulk and surface properties of Germanium for the use in next generation space solar cell devices. In two crystallization runs, Ge substrates with a wide doping concentration range from  $2 \times 10^{16}$  to  $1 \times 10^{17}$  at/cm<sup>3</sup> were produced. An in-situ plasma cleaning and passivation procedure for Ge wafers was developed applying H<sub>2</sub>/Ar plasma for 30 s and depositing an a-Si<sub>x</sub>C<sub>1-x</sub>:H passivation layer. For lowly doped samples champion lifetimes of  $\tau_{\text{eff}} > 300 \mu\text{s}$  could be achieved which is, considering the theoretical maximum value of  $400 \mu\text{s}$  and reported values in literature of well below  $300 \mu\text{s}$ , an excellent result. The achieved lifetimes correspond to  $\tau_{\text{bulk}}$  between 116 and 311  $\mu\text{s}$  depending on Ge bulk dopant concentration and surface recombination velocities ( $S_{\text{eff}}$ ) between 17 and 53 cm/s. After annealing at 400 °C the  $\tau_{\text{eff}}$  or the deposition of additional optical layers on top of the passivation layers lifetime values do not decrease or even slightly increase. Electron irradiation

experiments showed that with increased total electron fluences the lifetime values strongly decrease ending up at just 5  $\mu\text{s}$  for fluences of  $1 \times 10^{15}$  e/cm<sup>2</sup> independent of the substrate doping level. Layer composition, thickness or annealing seem to have no influence on the degradation behavior. However, as mobilities in Ge are very high, even this reduced lifetime values of just 5  $\mu\text{s}$  in lowly doped material correspond to diffusion lengths for minority carriers of around 200  $\mu\text{m}$  and can therefore lead to a significant efficiency improvement in the final solar cell.

#### ACKNOWLEDGEMENT

The authors would like to express their gratitude to F. Dimroth and E. Oliva at ISE for their support and input in many valuable discussions. This work has received funding from the European Union's Horizon 2020 research and innovation programme within the project SiLaSpaCe under grant agreement No 687336.

#### REFERENCES

- [1] Strobl, G. F. X. *et al.*, "European roadmap of multijunction solar cells and qualification status," in *Proceedings of the 21st European Photovoltaic Solar Energy Conference*, Hofmann, 2006, pp. 1793–1796.
- [2] N. E. Posthuma, G. Flamand, W. Geens, and J. Poortmans, "Surface passivation for germanium photovoltaic cells," *Sol. Energy Mater. Sol. Cells*, vol. 88, no. 1, pp. 37–45, 2005.
- [3] J. Fernandez, "Development of Germanium for TPV and High-Efficiency Multi-Junction Solar Cells," Dissertation, Fakultät für Physik, Konstanz, Universität, Konstanz, 2010.
- [4] J. Schmidt and A. G. Aberle, "Accurate method for the determination of bulk minority-carrier lifetimes of mono- and multicrystalline silicon wafers," *J. Appl. Phys.*, vol. 81, no. 9, pp. 6186–6199, 1997.
- [5] J. Fernández, F. Dimroth, E. Oliva, and A. W. Bett, "Development of germanium tpv cell technology," in 2007, pp. 516–519.